Systemic patterns of trabecular bone across the human and chimpanzee skeleton

Short title: Human and chimpanzee systemic trabecular patterns

Zewdi J. Tsegai [1], Matthew M. Skinner [2,1], Dieter H. Pahr [3], Jean-Jacques Hublin [1], Tracy L. Kivell [2, 1]

[1] Department of Human Evolution, Max Planck Institute for Evolutionary Anthropology

[2] Skeletal Biology Research Centre, School of Anthropology and Conservation, University of Kent

[3] Institute of Lightweight Design and Structural Biomechanics, Vienna University of Technology

Corresponding author:

Zewdi J. Tsegai

Max Planck Institute for Evolutionary Anthropology

Department of Human Evolution

Deutscher Platz 6

D-04103 Leipzig

Germany

zewdi_tsegai@eva.mpg.de

Abstract

Aspects of trabecular bone architecture are thought to reflect regional loading of the skeleton, and thus differ between primate taxa with different locomotor and postural modes. However, there are several systemic factors that affect bone structure that could contribute to, or be the primary factor determining, interspecific differences in bone structure. These systemic factors include differences in genetic regulation, sensitivity to loading, hormone levels, diet, and/or activity levels. Improved understanding of inter/intraspecific variability, and variability across the skeleton of an individual, is required to properly interpret potential functional signals present within trabecular structure. Using a whole-region method of analysis, we investigated trabecular structure throughout the skeleton of humans and chimpanzees. Trabecular bone volume fraction (BV/TV), degree of anisotropy (DA) and trabecular thickness (Tb.Th) were quantified from high resolution micro-computed tomographic scans of the humeral and femoral head, third metacarpal and third metatarsal head, distal tibia, talus and first thoracic vertebra. We find that BV/TV is, in most anatomical sites, significantly higher in chimpanzees than in humans, suggesting a systemic difference in trabecular structure unrelated to local loading regime. Differences in BV/TV between the forelimb and hindlimb do not clearly reflect differences in locomotor loading in the study taxa. There are no clear systemic differences between the taxa in DA and, as such, this parameter may reflect function and relate to differences in joint loading. This systemic approach reveals both the pattern of variability across the skeleton and between taxa, and helps identify those features of trabecular structure that may relate to joint function.

Keywords: Cancellous bone, Functional morphology, *Homo sapiens*, *Pan troglodytes*, Locomotion, Sedentism, Hominids

Introduction

The behaviour of extinct species can be reconstructed from plastic features of bony morphology that reflect an individual's behaviour during life (Ruff et al., 2006). Experimental studies have demonstrated the ability of bone to adapt to external loading (e.g. Lanyon, 1974; Robling et al., 2002; Mori et al., 2003; Pontzer et al., 2006; Barak et al., 2011; Wallace et al., 2013), a process often referred to as Wolff's Law (Wolff, 1986; Martin et al., 1998), or more generally as bone functional adaptation (Cowin, 2001; Ruff et al., 2006). Trabecular bone has potential for reconstructing the behaviour of fossil taxa (Kivell, 2016), as it remodels rapidly during life in response to strain (Ehrlich and Lanyon, 2002), in comparison to the slower rate of remodelling of cortical bone (Eriksen, 1986, 2010). Thus, the structure of trabecular bone could provide information about the mechanical loading history of a joint, in terms of both the load magnitude and direction. Studies among primates, including fossil specimens, have attempted to identify behavioural signals in trabecular structure with varying degrees of success (e.g. Fajardo and Müller, 2001; Ryan and Ketcham, 2002b; Griffin et al., 2010; Ryan and Shaw, 2012; Tsegai et al., 2013; Skinner et al., 2015; Stephens et al., 2016; Zeininger et al., 2016). The ultimate goal and framework within which these studies have been conducted is to first identify trabecular differences in living species that are related to behaviour, for example locomotor or manipulatory behaviours. Once this relationship between structure and behaviour has been established, similarities between the trabecular structure of fossil specimens and living taxa could be used to infer specific behaviours, or joint loading regimes, in fossil species.

However, the relationship between trabecular structure and behaviour in extant species is often unclear. For example, many trabecular bone analyses have focused on the primate proximal humerus (e.g. Fajardo and Müller, 2001; Fajardo et al., 2007; Ryan and Walker, 2010; Shaw and

Ryan, 2012; Scherf et al., 2013; Scherf et al., 2015) and, for historical reasons (Skedros and Baucom, 2007), the proximal femur (e.g. Fajardo and Müller, 2001; MacLatchy and Müller, 2002; Ryan and Ketcham, 2002a, b, 2005; Scherf, 2008; Ryan and Walker, 2010; Saparin et al., 2011; Ryan and Shaw, 2012; Shaw and Ryan, 2012). However, few of these studies have found clear differences in the trabecular structure of these joints that can be directly related to locomotor mode and predicted joint function. Where structural differences in trabecular architecture have been identified across locomotor groups, there is often no clear biomechanical explanation, and trabecular architecture is not always consistent with predictions based on biomechanical models. For example, studies of strepsirrhines have found that trabeculae within the femoral head was more uniformly oriented in vertical clinging and leaping species compared with slow climbing and/or quadrupedal taxa (MacLatchy and Müller, 2002; Ryan and Ketcham, 2002b, 2005). However, finite element analysis of the femoral head was unable to identify differences in bone strain at a range of load orientations in vertical clinging and leaping *Galago* compared to slow quadrupedal/climbing *Loris* (Ryan and van Rietbergen, 2005). This implies that different trabecular structures may be able to mitigate stress in similar ways, and that joint loading at the femoral (and potentially humeral) heads may actually be more similar than predicted across divergent locomotor modes (Ryan and van Rietbergen, 2005; Fajardo et al., 2007).

Since the first three-dimensional analysis of trabecular structure in primates (Fajardo and Müller, 2001), trabecular architecture has been described across a range of species and anatomical sites. This body of work has revealed particular interspecific patterns in the variation of trabecular structure, which suggests that any given species may have a similar trabecular structure across several elements of their skeleton. As a notable example, recent humans have been shown to

have low trabecular bone volume throughout the postcranial skeleton, including highly-loaded lower limb bones, such as the femur (e.g. Maga et al., 2006; Griffin et al., 2010; Tsegai et al., 2013; Chirchir et al., 2015; Ryan and Shaw, 2015; Saers et al., 2016; Stephens et al., 2016; Chirchir et al., 2017). In contrast, chimpanzees tend to have high bone volume across different skeletal elements in comparison to other hominoids (e.g. Maga et al., 2006; Griffin et al., 2010; Tsegai et al., 2013). Although few trabecular studies include bonobos, their metacarpals and metatarsals have the highest bone volume amongst the great apes (Griffin et al., 2010; Tsegai et al., 2013), which is not readily explained by variation in body size, locomotor mode, or activity level (Susman et al., 1980; Doran, 1992, 1993a). Although bone volume fraction is the trabecular parameter most strongly correlated with bone stiffness (Stauber et al., 2006; Maquer et al., 2015), it does not seem to correspond directly to predictions of joint loading based on locomotor mode.

There are several genetic and environmental factors, other than specific locomotor behaviours, that could have a systemic effect on bone remodelling and trabecular structure (Bertram and Swartz, 1991; Ruff et al., 2006; Kivell, 2016). Aspects of loading that are not evidently related to specific positional or locomotor behaviours include loading magnitude due to body mass (Doube et al., 2011; Fajardo et al., 2013; Ryan and Shaw, 2013), differences in loading frequency associated with overall activity levels (Lieberman, 1996), and other factors that may affect the frequency, magnitude or orientation(s) of load and thus potentially impact remodelling of both cortical and trabecular bone (Rubin and Lanyon, 1985; Frost, 1987; Skerry and Lanyon, 1995; Wallace et al., 2013). Genetic factors that might contribute to species-specific trabecular structure include hormonal differences or differences in bone regulation, even between closely related species (Lovejoy et al., 2003; Behringer et al., 2014a; Behringer et al., 2014b), between

males and females (Riggs and Melton, 1995; Reginster and Burlet, 2006; Eckstein et al., 2007) or at different life stages (Riggs and Melton, 1995; Tanck et al., 2001; Reginster and Burlet, 2006; Ryan and Krovitz, 2006; Gosman and Ketcham, 2009). These genetic differences may also manifest as phylogenetic differences in bone structure, unrelated to locomotor mode (Fajardo et al., 2013; Ryan and Shaw, 2013). Other aspects of the environment, such as diet and the intestinal microbiome, could also have a systemic effect on bone structure (Prentice, 1997; Shea et al., 2002; Cashman, 2007; Cao et al., 2009; Charles et al., 2015; McCabe et al., 2015). As the rate of remodelling of bone is higher during growth, behaviours during development may be more important for explaining trabecular morphology than those during adulthood (Bertram and Swartz, 1991; Pettersson et al., 2010). This is of particular relevance for African apes, as the percentage of knuckle-walking and suspension change significantly during development (Doran, 1992, 1997; Sarringhaus et al., 2014; Sarringhaus et al., 2016), although long bone cross-sectional geometry in African apes continues to change into adulthood and reflect locomotor behaviour at different life stages (Ruff et al., 2013; Sarringhaus et al., 2016; but see Demes et al., 1998; Demes et al., 2001; Lieberman et al., 2004; Carlson, 2005). Trabecular morphology may differ due to anatomical location (Morgan and Keaveny, 2001; Eckstein et al., 2007; Wallace et al., 2015); for example, distal limb elements may be adapted to have a lower bone mass (bone mineral density measured using pQCT and multiplied by joint size) and BV/TV than more proximal limb elements (Chirchir, 2015; Saers et al., 2016).

The absence of detailed locomotor, positional and biomechanical data on particular primate species may also contribute to limited identification of clear functional signals in trabecular bone. For example, accurate information on locomotor frequencies is rare, in part because several primate taxa are challenging to study in the wild due to lack of habituated populations,

rarity of the species itself, and/or high density forest cover (Crompton et al., 2010). Many species, especially hominoids, engage in multiple positional and locomotor behaviours (Hunt, 1991; Thorpe and Crompton, 2006; Myatt et al., 2011), beyond often over-simplified locomotor categories. Furthermore, due to the difficulty –both ethically and practically– of studying the biomechanics of locomotion in humans and especially non-human primates, there is little accurate biomechanical data concerning loading orientations and joint reaction forces to inform trabecular studies. Morphological differences related to locomotion have been investigated in primate taxa through finite element analysis (e.g. Ryan and van Rietbergen, 2005; Richmond, 2007; Nguyen et al., 2014). Although finite element analyses enable more informed predictions, they are often limited by a necessity to artificially reduce the complexity of the trabecular structure (due to computational limitations) and a lack of validation (Richmond et al., 2005; Ryan and van Rietbergen, 2005; Strait et al., 2005; Nguyen et al., 2014). Thus it is difficult to determine which behaviour, or combinations of behaviours, are reflected in trabecular bone structure.

To fully understand the functional significance of the trabecular bone structure of fossil hominins, we need to further explore variation in trabecular bone across the skeleton of living species. Previous studies have largely focused on one anatomical site (e.g. DeSilva and Devlin, 2012; Tsegai et al., 2013; Stephens et al., 2016) or region (Lazenby et al., 2011a; Schilling et al., 2014; Tsegai et al., 2017), or have been limited to comparisons between the humerus and femur (Fajardo and Müller, 2001; Ryan and Walker, 2010; Ryan and Shaw, 2012; Shaw and Ryan, 2012), and thus lack the context of how trabecular structure in any particular element or region might reflect, at least in part, a broader systemic pattern. Several recent studies have addressed the question of why previous comparative studies of trabecular bone have found notably gracile

bone in modern humans. Chirchir et al. (2015) conducted an analysis of trabecular structure across several skeletal elements in a sample of modern humans, fossil hominins and other extant primates, showing that gracile trabecular structure in humans is a relatively recent (i.e. Holocene) phenomenon. Ryan and Shaw (2015) further demonstrated, through a 3D volume of interest analysis of trabecular structure in the proximal femur of modern humans varying in subsistence strategies (foragers vs. agriculturalists), that gracile bone structure of recent humans is likely linked to a reduction in overall activity level with the adoption of agriculture. This gracilisation of the skeleton of agriculturalists is apparent across the lower limb, in the proximal and distal epiphyses of the femur and tibia, although all populations share a proximo-distal reduction in bone volume and increase in anisotropy (Saers et al., 2016). A similar pattern of gracilisation in recent humans, compared to a Neolithic population, is also present in the proximal humerus (Scherf et al., 2015). Chirchir et al. (2017) quantified trabecular bone fraction from pQCT data in the forelimb and hindlimb of five groups of modern humans, with a range of lifestyles, from foraging to industrial sedentary populations. This revealed a reduction in hindlimb robusticity with increased sedentism, and more variable changes in forelimb robusticity. Variability in trabecular architecture across the skeleton of recent humans has been documented, largely in the clinical literature. There is high intra-individual variability in trabecular structure, with low correlation between anatomical sites in several measures of trabecular architecture, quantified using 2D and 3D stereological methods (Amling et al., 1996; Parkinson and Fazzalari, 2003), pQCT (Groll et al., 1999; Chirchir, 2016), and microCT (Hildebrand et al., 1999; Ulrich et al., 1999; Eckstein et al., 2007). However, as yet, no study has conducted a comprehensive trabecular analysis, including parameters other than trabecular bone volume, across several skeletal elements in humans in comparative context with other primates. Thus, it remains

unknown how potential systemic patterns in trabecular bone might vary intraspecifically and interspecifically.

In this study we address this issue through quantification of trabecular bone volume fraction (BV/TV), degree of anisotropy (DA) and trabecular thickness (Tb.Th) in several anatomical sites within associated skeletons of recent humans and chimpanzees. Based on previous findings described above, we test three predictions: first, we predict that chimpanzees will have a higher BV/TV throughout the skeleton compared to humans (Maga et al., 2006; Griffin et al., 2010; Tsegai et al., 2013; Chirchir et al., 2015). Second, as humans and chimpanzees adopt locomotor behaviours that involve differential loading of the forelimb and hindlimb, we predict that BV/TV will be relatively similar across both limbs in chimpanzees, while BV/TV will be low across the forelimb compared to the hind limb in humans. Previous studies have demonstrated that humeral and femoral head trabecular structure does not reflect this difference in locomotor loading (Fajardo and Müller, 2001; Ryan and Walker, 2010; Shaw and Ryan, 2012), thus in this study we aim to test whether this pattern is consistent in other elements of the fore- and hindlimb. Third, as trabecular fabric has previously been associated with load direction and variability, we expect DA to differ between taxa in ways that reflect loading differences (Ryan and Ketcham, 2002b; Barak et al., 2013b; Su et al., 2013). Although Tb.Th is strongly correlated with body size (Doube et al., 2011; Barak et al., 2013a; Fajardo et al., 2013; Ryan and Shaw, 2013), it is also highly correlated with BV/TV (Barak et al., 2013a), and as such could parallel the systemic pattern of BV/TV. However, since the taxa in this study sample have a similar body mass, we predict that there will be no differences in trabecular thickness between these taxa, as has been found in general in previous studies (Cotter et al., 2009; Scherf et al., 2013; Ryan and Shaw, 2015; Zeininger et al., 2016; but see Barak et al., 2013b; Su and Carlson, 2017).

Methods

Sample

Trabecular bone structure was analysed in the skeletons of *Pan troglodytes* (N = 7) and recent *Homo sapiens* (N = 7) individuals. Full details of the study sample are shown in Table 1. All chimpanzee specimens belong to a single subspecies, *P. t. verus*, and were wild-collected skeletons from the Taï National Park, Republic of Côte d'Ivoire. The human sample was collected from two skeletal collections: one from a 19th century cemetery in Inden, Germany and the other from 13-15th century medieval cemeteries in Canterbury, UK. All specimens were free from external signs of pathology. Trabecular architecture was quantified in two anatomical locations in the forelimb (humeral head and third metacarpal head [MC3]), four anatomical sites in the hindlimb (femoral head, distal tibia, talus, and third metatarsal head [MT3]) and one site in the axial skeleton (first thoracic vertebra [T1]) (Fig. 1). These anatomical sites were chosen to include elements from both limbs, and an element from the axial skeleton that is less affected by differential loading of the fore- and hindlimb. We aimed to sample all bones of the forelimb and hindlimb from the same side, but when elements were not adequately preserved, all elements from either the forelimb or hindlimb were taken from the contralateral side where possible. For example, if the right femur was absent, then the femur, tibia, talus and MT3 were taken from the left side where possible.

Micro-CT scanning

All specimens were CT scanned using either a SkyScan 1173 or a BIR ACTIS 225/300 scanner housed at the Department of Human Evolution, Max Planck Institute for Evolutionary Anthropology (Leipzig, Germany). All scans were reconstructed as 16-bit tiff stacks with isotropic voxel sizes of 21-38 µm. All specimens were reoriented into standardised anatomical positions and were downsampled, due to computational constraints, using Avizo 6.3. Specimens

were analysed at a range of resolutions (25-45µm), with adequate representation of trabeculae as demonstrated by the relative resolution (4.25-9.83), which indicates how many pixels represent the average trabecular strut (Sode et al., 2008). Following this, all specimens were segmented using the Ray Casting Algorithm of Scherf and Tilgner (2009).

Trabecular bone quantification

Analysis of trabecular bone structure was conducted using an in-house script in medtool v3.9 (www.dr-pahr.at), following Gross et al. (2014). Morphological filters were used to automatically segment the cortical and trabecular bone, resulting in definition of three materials: (1) cortical bone, (2) trabecular bone and (3) air inside the bone (Fig. 2A). In this way, the trabecular bone throughout an entire region (or the whole bone, in the case of the talus) could be analysed. Tb.Th was calculated using the BoneJ plugin (v1.3.12; Doube et al., 2010) for ImageJ (v1.46r; Schneider et al., 2012) from the segmented trabecular only region (Fig. 2B). To quantify the other trabecular parameters in medtool (following protocols outlined in Gross et al., 2014), a 2.5mm background grid was applied to each specimen, and a 5mm spherical volume of interest was used to measure BV/TV at each node of the background grid. A 3D tetrahedral mesh was created of the inner region of the bone (Fig. 2C), to which each node was assigned a BV/TV value (Fig. 2D) interpolated from the background grid. A mesh size of 1mm was used for the larger specimens (humeral head, femoral head, distal tibia, and talus) and a mesh size of 0.5mm for the smaller specimens (MC3, MT3, and T1). As the background grid size was constant for the sample, the results are independent of mesh size. The overall BV/TV was calculated as the mean of all elements in the 3D region of interest (ROI; see below). The mean intercept length method was used to calculate the local fabric tensor for each tetrahedron and these were normalised by the determinants (Luisier et al., 2014). Similar to BV/TV, an arithmetic mean of

all of the second order fabric tensors was computed within the ROI. The DA was calculated as the DA = 1 – [smallest eigenvalue/largest eigenvalue], such that a DA of 1 represents "complete" anisotropy (i.e. all trabeculae are aligned, and there are no crossing trabeculae) and a DA of 0 reflects complete isotropy (i.e. there is no preferential alignment of trabeculae). Often the DA is bound between a DA of 1 representing isotropy and a DA > 1 representing increasing anisotropy, however here we use an alternative, "normalised" DA.

In both humans and chimpanzees trabecular bone of the long bone epiphyses extends beyond the epiphysis and into the shaft. As such, the ROIs for long bones were defined in order to sample as much of the trabecular bone-filled region as possible, which could potentially contribute to systemic differences in trabecular structure. For each skeletal element the ROI was defined as follows (Fig. 1). For the proximal humerus, this was defined as the point where curvature of the humeral head begins to expand from the shaft both medially and laterally (Fig. 1A). In the proximal femur, the femoral head was extracted with the inferior margin being at the most inferior point of the femoral head and the medial margin at the most medial point of the femoral head (Fig. 1B). In the proximal femur, it was only possible to sample the femoral head, and small region of the femoral neck, due to computational constraints in processing large data sets. The ROI in the distal tibia was defined distally where curvature of the shaft begins in both medial and anterior views, which is at the proximal extent of the fibular notch (Fig. 1C). In the MC3 and MT3, the distal end (head) was defined as the point at which the shaft curves laterally in palmar/plantar view (Fig. 1D & E). In the T1, only the trabeculae in the vertebral body were quantified (Fig. 1F). For the talus the trabecular bone in the entire element was quantified. Identification of homologous regions is complex due to the potential effect of differences in location and size of the region being analysed. For example, sometimes dramatic differences in

quantification of trabecular bone structure have been found with variation in position or size of small volumes of interest within a bone or epiphysis (Fajardo and Müller, 2001; Kivell et al., 2011; Lazenby et al., 2011b). Here, our 3D ROI includes a much larger region of trabecular structure (e.g. the entire epiphysis), but quantified values may also be affected by how the ROI is defined between taxa. Therefore, a test of intra-observer error was conducted for the humerus and tibia of one human and one chimpanzee, with the ROI defined five times on five consecutive days. The percentage difference in BV/TV compared to the original quantified value, ranged from -0.97% to 0.22% for the humerus and from -2.29% to 0.73% for the tibia.

Statistical analysis

Statistical analysis was conducted using R v3.3.2 (R Core Team, 2016) and ggplot2 (Wickham, 2009) for plot generation. Due to small sample sizes non-parametric tests were used. Taxonomic differences in trabecular structure at each anatomical site were tested for using Mann-Whitney U tests between taxa. To identify systemic patterns within species, Friedman tests were used to identify whether there were overall significant differences between the ranks of anatomical sites in humans and in chimpanzees. Following the results of the Friedman tests, Wilcoxon exact tests with p-values corrected with a post-hoc Bonferroni adjustment, were used to identify significant pairwise differences between anatomical sites within humans and within chimpanzees. Differences in the systemic pattern between taxa were identified by comparing the results of within-species Wilcoxon exact tests. To identify correlations between trabecular parameters in different regions within humans and within chimpanzees. Spearman's correlation test was used with p-values corrected with a post-hoc Bonferroni adjustment. For all statistical tests a p-value < 0.05 was considered significant.

Results

Taxonomic differences

Means and standard deviations of trabecular parameters in each anatomical region and results of Mann-Whitney U tests for significant differences between species are shown in Table 2. Figure 3 shows box-and-whisker plots of the results for each taxon. There were no significant differences in Tb.Th between chimpanzees and humans in any anatomical region. Chimpanzees had significantly higher BV/TV than humans in the humeral, femoral, and MT3 heads as well as the talus. Chimpanzees also had significantly more anisotropic trabeculae in the humeral head and T1, and less anisotropic trabeculae in the talus and MT3.

Taxonomic differences in the patterning of BV/TV are further illustrated in Figure 4, where the BV/TV values are shown for each individual. In one human individual BV/TV values were much higher in every anatomical region, and this is the only individual that overlapped with chimpanzees in humeral, metatarsal, femoral, and talar BV/TV. Excluding this specimen from the statistical comparisons presented above led to significantly lower BV/TV in the human MC3 ($p = 0.03$), while the BV/TV values in the thoracic vertebra and tibia approached significance ($p = 0.05$).

Intraspecific and interspecific systemic patterns

Comparisons of trabecular structure within individuals are presented in Table 3, as the mean rank of each element for each trabecular parameter. This demonstrates the systemic pattern of trabecular bone structure within each taxon, with elements having a higher mean rank indicating generally higher values in that anatomical region across individuals. Across both chimpanzees and humans, all hindlimb elements, except for the MT3, had a higher mean rank for Tb.Th than

the forelimb and axial elements, and the humerus had a higher mean rank for Tb.Th than the metacarpal. In chimpanzees, the order of mean ranks of the different anatomical sites for BV/TV was similar to that of Tb.Th. The only difference was a switch between the humerus and the T1. In humans, the ranks of anatomical sites for BV/TV followed the pattern for Tb.Th less closely. Notably, the humerus was the lowest ranking element for BV/TV in humans. The mean ranks of DA differed between the taxa. Within the hindlimb of chimpanzees, the DA had the highest mean rank in the tibia, MT3 and femur, with the talus having the most isotropic trabeculae. The pattern in humans differed from that of chimpanzees in that the MT3 had a higher DA rank compared to the other hindlimb anatomical sites. In the forelimb, the MC3 had a higher mean rank for DA than the humerus in both taxa.

Results of Friedman tests (Table 3) indicated the presence of significant differences between ranks of anatomical sites in all three trabecular parameters in both humans and chimpanzees. Post-hoc Wilcoxon test comparisons with a Bonferroni adjustment are shown in Table 4. For Tb.Th (Table 4), significant differences were largely due to thicker trabecular bone in the femur, tibia and talus compared to other elements in both taxa. The humerus had significantly thicker trabeculae than the MT3 in humans, and both the MC3 and MT3 in chimpanzees. Significant differences in BV/TV between elements were largely due to low BV/TV in the human humerus and to high BV/TV in the chimpanzee femur and talus (Table 4). Significant differences in DA were largely due to high DA in the tibia and low DA in the talus in chimpanzees. In humans, most significant differences were due to the high DA of the MT3.

Trabecular correlations between anatomical sites

Spearman's correlation tests, to identify whether trabecular parameters were correlated between anatomical sites within each taxon, revealed only two significant correlations. In chimpanzees,

there was a significant correlation in Tb.Th between the humerus and femur ($r = 0.96$, $p = 0.01$) and between the talus and MT3 ($r = 1.00$, $p < 0.01$). There were no significant correlations between anatomical sites in humans.

Discussion

This study provides the first comprehensive 3D analysis of potential systemic patterns in trabecular architecture across the skeleton of humans and chimpanzees using a whole bone/region approach. We find both similarities and differences in regional patterning of trabecular structure across individuals and between taxa. Due to substantial variation in the morphology of the bones/epiphyses included in this study, direct comparison of trabecular bone architecture between anatomical sites is complex, as it may be influenced by factors such as articular surface area or the proximo-distal location of the element (Chirchir, 2015; Saers et al., 2016; for cortical bone see Lieberman et al., 2003). However, by identifying both shared and distinct systemic patterns of trabecular structure, relative (rather than absolute) comparisons can be made across anatomical sites and between taxa. In this comparative context, we find that the systemic pattern of BV/TV, Tb.Th and DA differs between chimpanzees and humans. However, this pattern is not always consistent across the skeleton, or clearly related to joint function based on predicted loading during locomotion.

Taxonomic differences in BV/TV

Recent modern humans have been found to have a lower BV/TV than non-human primates in various anatomical sites (e.g. Maga et al., 2006; Griffin et al., 2010; Shaw and Ryan, 2012; Scherf et al., 2013; Tsegai et al., 2013; Chichir et al., 2015; Ryan and Shaw, 2015), thus we predicted that chimpanzees would have higher BV/TV in all anatomical regions sampled in our study. We find general support for this hypothesis, with chimpanzees having significantly higher

BV/TV than humans in the humeral, femoral and MT3 heads and the talus, and higher mean BV/TV values, but not significantly so, in the distal tibia, MC3 and T1. Thus, using a whole-bone/region approach across the skeletons of the same individuals, our results provide further support of a general pattern of higher BV/TV in chimpanzees compared with humans documented in previous studies.

Recent trabecular analyses have demonstrated the potential influence of activity levels on trabecular architecture in modern humans, including BV/TV quantified from micro-CT scans or converted from pQCT measures of volumetric mineral density (Chirchir et al., 2015; Ryan and Shaw, 2015; Scherf et al., 2015; Saers et al., 2016; Chirchir et al., 2017). Recent modern humans have lower BV/TV, calculated from pQCT scans, in both the upper and lower limb compared to early modern humans and other fossil hominins, including *H. neanderthalensis* and members of *Australopithecus* (Chirchir et al., 2015). The trabecular architecture in the centre of the proximal humerus of recent modern humans is weaker (e.g. lower BV/TV and Tb.Th) than in Neolithic modern humans (5,700-4,900BP) (Scherf et al., 2015). The timing of this reduction in BV/TV may be related to changes in overall activity level, with recent mobile foragers having stronger bone (higher BV/TV, higher Tb.Th, lower bone surface to volume ratio) in the proximal and distal femur and tibia compared to recent sedentary agriculturalists (Ryan and Shaw, 2015; Saers et al., 2016) and differences in trabecular BV/TV, quantified using pQCT, in particular of the lower limb, can be related to subsistence strategy in recent populations (Chirchir et al., 2017).

In the sample included in this study, one human individual has higher BV/TV in every region of the skeleton, which overlaps with chimpanzees in all anatomical locations. Unfortunately, no historical information is available regarding the activity level or occupation of this individual. However, it provides further support for a systemic pattern of trabecular BV/TV that could be

related to systemic factors, such as higher activity levels promoting bone remodelling throughout the skeleton (Lieberman, 1996). Across canids, felids and cercopithecines, species with longer travel distances have a higher relative trabecular bone mass, quantified from pQCT, than species with shorter travel distances, indicating the potential influence of overall activity on trabecular structure in a range of taxa (Chirchir et al., 2016a).

An explanation is not readily available for the high BV/TV in chimpanzees, in comparison to both active populations of humans and other primate taxa. In the femoral head, chimpanzees have higher BV/TV than closely related *Gorilla* and modern humans, having the highest BV/TV amongst 32 primate taxa (Ryan and Shaw, 2013), and when compared to humans with different subsistence strategies (Ryan and Shaw, 2015). In the humeral head, chimpanzees have higher BV/TV than Neolithic modern humans, recent modern populations and *Pongo* (Scherf et al., 2013; Scherf et al., 2015). Thus, activity levels alone may not explain the systemic difference in BV/TV between humans, chimpanzees, and other primate taxa. This is of particular importance for functional inferences drawn from trabecular structure in fossil hominins, where some anatomical regions or isolated specimens are also characterised by high trabecular BV/TV, similar to or higher than that of chimpanzees (Barak et al., 2013b; Chirchir et al., 2015; Skinner et al., 2015).

Functional signals in systemic patterns of BV/TV

We predicted that the patterns of trabecular BV/TV in the forelimb and hindlimb of chimpanzees and humans would reflect differential loading during locomotion, such that quadrupedal chimpanzees would have more similar BV/TV values in the forelimb and hindlimb, whereas bipedal humans would have higher BV/TV in the hindlimb elements. It is important to make comparisons between elements at a similar anatomical location due to the proximo-distal

decrease in trabecular bone mass (bone mineral density measured using pQCT and multiplied by joint size) and BV/TV in hominoids and populations of humans with different subsistence strategies (Chirchir, 2015; Saers et al., 2016). Thus, here we discuss differences between the humeral and femoral head and between the MC3 and MT3 head.

We find that both chimpanzees and humans have significantly higher BV/TV in the femoral head compared with the humeral head. This is consistent with previous comparisons of trabecular bone in the humerus and femur in a range of anthropoid species, where all individuals (Fajardo and Müller, 2001; Ryan and Walker, 2010), or the majority of individuals (Shaw and Ryan, 2012), were found to have higher BV/TV in the femoral head compared to the humeral head. Mean trabecular BV/TV, derived from micro-CT and pQCT, is higher in the femoral head compared to the humeral head in extant chimpanzees, modern humans, early modern humans, and *H. neanderthalensis* (but not in *Australopithecus africanus*) (Chirchir et al., 2015; Chirchir, 2016), but this difference is not significant in modern humans (Chirchir, 2016). Previous analyses of proximal femoral trabecular properties in humans, although not incorporating the humeral head, or the same anatomical sites as the present study, have also found relatively high trabecular BV/TV in the femoral neck (Amling et al., 1996; Eckstein et al., 2007 [in men but not women]) and femoral head (Hildebrand et al., 1999; Ulrich et al., 1999; Parkinson and Fazzalari, 2003) compared to other anatomical sites analysed (but see Chirchir, 2016).

However, the skeletal pattern is more complex when the BV/TV of other anatomical sites is considered. We find that, compared to other anatomical regions, chimpanzees have very high femoral BV/TV, having the highest mean rank of all anatomical sites, whereas in humans femoral BV/TV ranks lower than the talus. In contrast, humeral BV/TV in humans has the lowest mean rank, whereas in chimpanzees it ranks above the MT3 and MC3. Thus, chimpanzees have

relatively high femoral BV/TV and humans have very low humeral BV/TV, compared to other anatomical sites. This finding supports our prediction that trabecular BV/TV would reflect reduced loading of the human forelimb, but the pattern in chimpanzees does not support our prediction of similar loading between the two limbs. This could be due to the 'hindlimb driven' quadrupedal locomotion of chimpanzees, and other primate taxa, whereby the hindlimb experiences greater vertical reaction forces than the forelimb, and propulsion is driven by the hindlimb (Kimura et al., 1979; Demes et al., 1994). Thus, high BV/TV in femoral head of chimpanzees and other primate taxa may reflect this difference in function of the hindlimb during quadrupedal locomotion.

Comparisons between the MC3 and MT3 also do not support the hypothesis of higher BV/TV in the hindlimb of humans and more similar BV/TV between the forelimb and hindlimb of chimpanzees. On average, both humans and chimpanzees have higher BV/TV in the MC3 compared to the MT3, and, in contrast to our predictions, this pattern is more pronounced in humans. In all human specimens in the study sample, and in 57% of the chimpanzees, the MC3 has higher BV/TV than the MT3, with this difference being significant in humans. This is consistent with previous findings, where on average bone density in humans is higher in the metacarpal head while in chimpanzees it is higher in the metatarsal head (Chirchir et al., 2015). Thus, comparisons of BV/TV (derived both from micro-CT and pQCT scans) between the MT3 and MC3 does not reflect higher loading of the human hindlimb and more equal loading of the forelimb and hindlimb in chimpanzees. These patterns identified between the femoral and humeral heads, the MC3 and MT3, and throughout the skeleton may reflect the complex relationship between mechanical load, activity level, and anatomical site (Judex et al., 2004; Wallace et al., 2012; Wallace et al., 2013; Wallace et al., 2015).

Taxonomic differences and systemic patterning of DA and Tb.Th

Trabecular structure across the skeleton of humans and chimpanzees supports our prediction that there would be no consistent taxonomic differences in DA. We found no consistent pattern in DA values across the seven anatomical regions within each species. Humans had significantly more anisotropic trabeculae in the talus and MT3, and significantly more isotropic trabeculae in the humeral head and T1 compared to chimpanzees. This variability between taxa and anatomical sites may indicate that DA is primarily reflecting differences in joint loading (see below).

Tb.Th has previously been found to scale with body size in a range of primate taxa and anatomical sites (Doube et al., 2011; Barak et al., 2013a; Fajardo et al., 2013; Ryan & Shaw, 2013), but also to correlate with BV/TV (Barak et al., 2013a). Here, in support of our prediction, we found no significant differences in absolute Tb.Th between humans and chimpanzees. Considering the smaller body size of chimpanzees, this indicates that they have relatively thick trabeculae compared to humans, however due to the small difference in body size this is unlikely to lead to significant differences. We did, however, find that the systemic pattern of Tb.Th followed a similar pattern in both taxa, being generally higher in the hindlimb (femoral head, talus and distal tibia) and lower in the forelimb (humerus and MC3) in both taxa. This is supported by previous comparisons of Tb.Th between the humerus and femur, which found thicker femoral trabeculae in most taxa/individuals (Ryan and Walker, 2010; Shaw and Ryan, 2012; Ryan and Shaw, 2013). However, the MT3 had thin trabecular bone compared to the rest of the hindlimb in both humans and chimpanzees, despite different loading regimes between these two taxa. Differences in BV/TV, but not Tb.Th, indicate potential differences in trabecular number (Tb.N) between these taxa. Previous studies have found differences in Tb.N between

humans and chimpanzees (e.g. distal tibia: Su, 2011; Barak et al., 2013b; vertebra: Cotter et al., 2009; femoral head: Ryan and Shaw, 2012; Shaw and Ryan, 2012; humeral head: Ryan and Shaw, 2012; Shaw and Ryan, 2012; Scherf et al., 2013) with chimpanzees having more numerous trabeculae, although this is not the case for the talus (Su, 2011; DeSilva and Devlin, 2012) or calcaneus (Kuo et al., 2013; Zeininger et al., 2016).

Functional signals in systemic patterns of DA

The degree of anisotropy of trabeculae, and other related measures such as primary trabecular orientation and elongation index, are often able to distinguish between locomotor mode, especially when comparisons are made between different regions of an epiphysis (e.g. MacLatchy and Müller, 2002; Ryan and Ketcham, 2002b; Maga et al., 2006; Griffin et al., 2010; Hebert et al., 2012; Barak et al., 2013b; Su et al., 2013; Zeininger et al., 2016; Su and Carlson, 2017). However, not all trabecular analyses have identified differences in DA or orientation-based variables between locomotor groups (e.g. Fajardo et al., 2007; Kuo et al., 2013). In general, DA is thought to reflect the range of joint positions in which a joint experiences high loads, with more uniformly aligned trabeculae being associated with more stereotypical load orientations, and more isotropic trabeculae with a greater range of adopted joint positions (Fajardo and Müller, 2001; Ryan and Ketcham, 2002b). There is evidence of a systemic pattern in a proximo-distal increase in DA in the human femur and tibia (Saers et al., 2016), which is also found in the present study between the proximal femur and distal tibia. However, this could be a structural adaptation to the proximo-distal reduction in BV/TV, or could be related to other factors, such as differences in gross morphology, and thus loading stereotypy, between the femur and tibia (Saers et al., 2016).

We predicted that DA in the hindlimb and humeral head of chimpanzees would reflect differences in loading between the study taxa. In general, humans experience more stereotypical loading of the hindlimb than chimpanzees, whose locomotor repertoire includes knuckle-walking quadrupedalism and several arboreal behaviours (e.g. climbing, clambering and suspension) that require a greater range of joint positions (Hunt, 1991; Doran, 1992, 1993b, 1997; Sarringhaus et al., 2014). We find some support for this prediction. The hindlimb of humans has significantly higher DA in the MT3 head and talus compared to chimpanzees, perhaps reflecting the more stereotypical loading during bipedalism, especially in the foot. Moreover, DA is significantly higher in the MT3 than the MC3 of humans, but not in chimpanzees. However, this is not the case for the distal tibia, where chimpanzees have higher DA (contrary to Barak et al., 2013b). In the chimpanzee forelimb, we find significantly higher DA in the humeral head (contrary to Scherf et al., 2013), and higher mean DA in the metacarpal head (supporting the findings of Tsegai et al., 2013; Chirchir et al., 2016b) compared to humans. In the T1 we find significantly higher DA in chimpanzees compared to humans. A previous analysis of DA in eighth thoracic vertebra found no significant difference in DA between chimpanzees and humans, but did identify a negative correlation between BV/TV and DA in humans, which was absent in non-human apes (Cotter et al., 2009), indicating a complex interplay between these trabecular parameters in the spinal column.

Although DA appears to correspond with the type of loading in some anatomical sites, other anatomical areas do not (e.g. the humeral head and distal tibia), nor do they always support the findings of previous studies. This may be related to the whole-region method applied in this study, where trabecular bone from a larger region is quantified, in comparison to previous studies where DA was measured in smaller sub-regions (e.g. volume of interest). Whether trabecular

alignment in a small subregion, or in an entire region, is a better indicator of overall loading is unclear. Another potential explanation, is that our predictions of joint loading are often oversimplified, and the impact of different behaviours on bone structure is unknown. For example, a lower DA might have been expected for the chimpanzee humeral head, based on their adoption of a range of arboreal behaviours and thus varied load orientations. However, knuckle-walking is the most frequent locomotor behaviour used by adult chimpanzees (Doran, 1992; Sarringhaus et al., 2014), and as such, may contribute more to trabecular anisotropy than less frequent arboreal locomotor bouts.

Trabecular structure and articular morphology

Comparisons of trabecular bone structure between anatomical regions, or indeed of the same anatomical region between different taxa, are potentially influenced by differences in the gross morphology of the articular region, and by articular function. Primate taxa differ in relative articular surface area and absolute articular size, due to differences in both the magnitude of load and the range of joint excursion, which can be related to locomotor mode (Ruff, 1988; Godfrey et al., 1991; Ruff and Runestad, 1992; Godfrey et al., 1995; Ruff, 2002). Moreover, the relationship between articular surface area and joint mobility may differ between joint types; for example in a ball-and-socket joint, an increase in surface area may have more of an impact on joint mobility than in a hinge joint (Ruff, 2002). Although our discussion has focused largely on the comparative context, i.e. differences in the systemic pattern between humans and chimpanzees, it is important to recognise the potential impact of these aspects of external joint morphology on the findings of this study. It is beyond the scope of the present study to explore this further, however, it is an important and relatively unexplored area of trabecular research (but see Rafferty and Ruff, 1994). Future research into systemic patterns of trabecular structure

should further investigate the relationship between trabecular morphology and external articular morphology, both within and between taxa.

Conclusion

Here we demonstrate that an understanding of the way in which trabecular bone varies across the skeleton can have important implications for inferring joint load, function, and ultimately behaviour, from trabecular structure. Chimpanzees and humans have systemically different trabecular BV/TV throughout their skeleton, such that humans (except for one individual within our sample) had lower BV/TV in all anatomical regions compared with chimpanzees. However, differences in BV/TV between the humeral and femoral head and the MC3 and MT3 do not directly reflect predicted differences in loading of the fore- and hindlimb in each taxon. Rather, overall BV/TV may be driven by other factors, such as overall activity level (Ryan and Shaw, 2015). Mean Tb.Th values across the skeleton do not differ significantly between chimpanzees and humans, and trabeculae are generally thicker in the hindlimb compared with the forelimb in both taxa. These systemic patterns must be considered when inferring the magnitude of joint load in any one skeletal area (e.g. high BV/TV may not necessarily reflect solely higher load/activity levels). This is particularly true, but also especially challenging, when inferring function in fossil taxa when only isolated elements are preserved, and thus potential systemic patterns are unknown. In contrast to BV/TV, the degree to which trabeculae are preferentially oriented (DA) did not differ consistently across the skeleton within chimpanzees or humans. Although the pattern of DA across different skeletal elements did not always fit our predictions, the pattern suggests that trabecular alignment may more directly reflect differences in the magnitude and direction of joint loading, and thus behaviour, than BV/TV (and Tb.Th).

Author contributions

Concept/design: ZJT, MMS, JJH, TLK; Acquisition of data: ZJT; Data analysis/interpretation: ZJT, MMS, DHP, TLK; Drafting and revision of the manuscript: ZJT, MMS, DHP, JJH, TLK; Approval of the article: ZJT, MMS, DHP, JJH, TLK

Acknowledgements

This research was supported by the Max Planck Society (ZJT, TLK, MMS and JJH) and European Research Council Starting Grant #336301 (TLK and MMS). For access to specimens we thank Christophe Boesch (Max Planck Institute for Evolutionary Anthropology), Birgit Grosskopf (Georg-August-Universität Göttingen), and Chris Deter and Patrick Mahoney (University of Kent). For scanning assistance we thank David Plotzki, Patrick Schönfeld and Heiko Temming. We thank Nicholas Stephens for discussion and three anonymous reviewers, whose comments greatly improved this manuscript.

References

Amling M, Herden S, Pösl M, Hahn M, Ritzel H, Delling G (1996) Heterogeneity of the skeleton: Comparison of the trabecular microarchitecture of the spine, the iliac crest, the femur, and the calcaneus. *J Bone Miner Res,* **11,** 36-45.

Barak MM, Lieberman DE, Hublin J-J (2011) A Wolff in sheep's clothing: Trabecular bone adaptation in response to changes in joint loading orientation. *Bone,* **49,** 1141-1151.

Barak MM, Lieberman DE, Hublin J-J (2013a) Of mice, rats and men: trabecular bone architecture in mammals scales to body mass with negative allometry. *J Struct Biol,* **183,** 123-131.

Barak MM, Lieberman DE, Raichlen D, Pontzer H, Warrener AG, Hublin J-J (2013b) Trabecular evidence for a human-like gait in *Australopithecus africanus*. *PLoS ONE,* **8,** e77687.

Behringer V, Deschner T, Deimel C, Stevens JMG, Hohmann G (2014a) Age-related changes in urinary testosterone levels suggest differences in puberty onset and divergent life history strategies in bonobos and chimpanzees. *Horm Behav,* **66,** 525 - 533.

Behringer V, Deschner T, Murtagh R, Stevens JMG, Hohmann G (2014b) In bonobos and chimpanzees age-related changes in urinary thyroid hormones indicate heterochrony in their development. *Am J Phys Anthropol,* **153,** 75-76.

Bertram JE, Swartz SM (1991) The 'law of bone transformation': a case of crying Wolff? *Biol Rev Camb Philos Soc,* **66,** 245-273.

Cao JJ, Gregoire BR, Gao H (2009) High-fat diet decreases cancellous bone mass but has no effect on cortical bone mass in the tibia in mice. *Bone,* **44,** 1097-1104.

Carlson KJ (2005) Investigating the form-function interface in African apes: Relationships between principal moments of area and positional behaviors in femoral and humeral diaphyses. *Am J Phys Anthropol,* **127,** 312-334.

Cashman KD (2007) Diet, Nutrition, and Bone Health. *The Journal of Nutrition,* **137,** 2507S-2512S.

Charles JF, Ermann J, Aliprantis AO (2015) The intestinal microbiome and skeletal fitness: Connecting bugs and bones. *Clin Immunol,* **159,** 163-9.

Chirchir H (2015) A comparative study of trabecular bone mass distribution in cursorial and non-cursorial limb joints. *Anat Rec,* **298,** 797-809.

Chirchir H (2016) Limited trabecular bone density heterogeneity in the human skeleton. *Anat Res Int,* **2016,** 7.

Chirchir H, Kivell TL, Ruff CB, et al. (2015) Recent origin of low trabecular bone density in modern humans. *Proc Natl Acad Sci U S A,* **112,** 366-371.

Chirchir H, Ruff CB, Helgen KM, Potts R (2016a) Trabecular bone mass and daily travel distance in mammals. *FASEB J,* **30,** 779.15.

Chirchir H, Ruff CB, Junno J-A, Potts R (2017) Low trabecular bone density in recent sedentary modern humans. *Am J Phys Anthropol,* **162,** 550-560.

Chirchir H, Zeininger A, Nakatsukasa M, Ketcham RA, Richmond BG (2016b) Does trabecular bone structure within the metacarpal heads of primates vary with hand posture? *C R Palevol*.

Cotter MM, Simpson SW, Latimer BM, Hernandez CJ (2009) Trabecular microarchitecture of hominoid thoracic vertebrae. *Anat Rec,* **292,** 1098-1106.

Cowin SC (2001) The false premise in Wolff's Law. In *Bone Mechanics Handbook, Second Edition* (ed Cowin SC). Boca Raton: CRC Press.

Crompton RH, Sellers WI, Thorpe SKS (2010) Arboreality, terrestriality and bipedalism. *Philos Trans R Soc Lond B Biol Sci,* **365,** 3301-3314.

Demes B, Larson SG, Stern JT, Jungers WL, Biknevicius AR, Schmitt D (1994) The kinetics of primate quadrupedalism: "hindlimb drive" reconsidered. *J Hum Evol,* **26,** 353-374.

Demes B, Qin YX, Stern JT, Larson SG, Rubin CT (2001) Patterns of strain in the macaque tibia during functional activity. *Am J Phys Anthropol,* **116,** 257-265.

Demes B, Stern JT, Jr., Hausman MR, Larson SG, McLeod KJ, Rubin CT (1998) Patterns of strain in the macaque ulna during functional activity. *Am J Phys Anthropol,* **106,** 87-100.

DeSilva JM, Devlin MJ (2012) A comparative study of the trabecular bony architecture of the talus in humans, non-human primates, and *Australopithecus*. *J Hum Evol,* **63,** 536-551.

Doran DM (1992) The ontogeny of chimpanzee and pygmy chimpanzee locomotor behavior: A case study of paedomorphism and its behavioral correlates. *J Hum Evol,* **23,** 139-157.

Doran DM (1993a) Comparative locomotor behavior of chimpanzees and bonobos: The influence of morphology on locomotion. *Am J Phys Anthropol,* **91,** 83-98.

Doran DM (1993b) Sex differences in adult chimpanzee positional behavior: The influence of body size on locomotion and posture. *Am J Phys Anthropol,* **91,** 99-115.

Doran DM (1997) Ontogeny of locomotion in mountain gorillas and chimpanzees. *J Hum Evol,* **32,** 323-344.

Doube M, Kłosowski MM, Arganda-Carreras I, et al. (2010) BoneJ: Free and extensible bone image analysis in ImageJ. *Bone,* **47,** 1076-1079.

Doube M, Klosowski MM, Wiktorowicz-Conroy AM, Hutchinson JR, Shefelbine SJ (2011) Trabecular bone scales allometrically in mammals and birds. *Proc Biol Sci,* **278,** 3067-73.

Eckstein F, Matsuura M, Kuhn V, et al. (2007) Sex differences of human trabecular bone microstructure in aging are site-dependent. *J Bone Miner Res,* **22,** 817-824.

Ehrlich PJ, Lanyon LE (2002) Mechanical strain and bone cell function: A review. *Osteoporosis Int,* **13,** 688-700.

Eriksen EF (1986) Normal and pathological remodeling of human trabecular bone: three dimensional reconstruction of the remodeling sequence in normals and in metabolic bone disease. *Endocr Rev,* **7,** 379-408.

Eriksen EF (2010) Cellular mechanisms of bone remodeling. *Rev Endocr Metab Disord,* **11,** 219-227.

Fajardo RJ, Desilva JM, Manoharan RK, Schmitz JE, Maclatchy LM, Bouxsein ML (2013) Lumbar vertebral body bone microstructural scaling in small to medium-sized strepsirhines. *Anat Rec,* **296,** 210-226.

Fajardo RJ, Müller R (2001) Three-dimensional analysis of nonhuman primate trabecular architecture using micro-computed tomography. *Am J Phys Anthropol,* **115,** 327-336.

Fajardo RJ, Müller R, Ketcham RA, Colbert M (2007) Nonhuman anthropoid primate femoral neck trabecular architecture and its relationship to locomotor mode. *Anat Rec,* **290,** 422-436.

Frost HM (1987) Bone "mass" and the "mechanostat": A proposal. *Anat Rec,* **219,** 1-9.

Godfrey L, Sutherland M, Boy D, Gomberg N (1991) Scaling of limb joint surface areas in anthropoid primates and other mammals. *Journal of Zoology,* **223,** 603-625.

Godfrey LR, Sutherland MR, Paine RR, Williams FL, Boy DS, Vuillaume-Randriamanantena M (1995) Limb joint surface areas and their ratios in Malagasy lemurs and other mammals. *Am J Phys Anthropol,* **97,** 11-36.

Gosman JH, Ketcham RA (2009) Patterns in ontogeny of human trabecular bone from SunWatch Village in the Prehistoric Ohio Valley: General features of microarchitectural change. *Am J Phys Anthropol,* **138,** 318-332.

Griffin NL, D'Août K, Ryan TM, Richmond BG, Ketcham RA, Postnov A (2010) Comparative forefoot trabecular bone architecture in extant hominids. *J Hum Evol,* **59,** 202-213.

Groll O, Lochmuller EM, Bachmeier M, Willnecker J, Eckstein F (1999) Precision and intersite correlation of bone densitometry at the radius, tibia and femur with peripheral quantitative CT. *Skeletal Radiol,* **28,** 696-702.

Gross T, Kivell TL, Skinner MM, Nguyen NH, Pahr DH (2014) A CT-image-based framework for the holistic analysis of cortical and trabecular bone morphology. *Palaeontol Electron,* **17,** 13.

Hebert D, Lebrun R, Marivaux L (2012) Comparative three-dimensional structure of the trabecular bone in the talus of primates and its relationship to ankle joint loads generated during locomotion. *Anat Rec,* **295,** 2069-88.

Hildebrand T, Laib A, Müller R, Dequeker J, Rüegsegger P (1999) Direct three-dimensional morphometric analysis of human cancellous bone: microstructural data from spine, femur, iliac crest, and calcaneus. *J Bone Miner Res,* **14,** 1167-1174.

Hunt KD (1991) Positional behavior in the Hominoidea. *Int J Primatol,* **12,** 95-118.

Judex S, Garman R, Squire M, Donahue L-R, Rubin C (2004) Genetically based influences on the site-specific regulation of trabecular and cortical bone morphology. *J Bone Miner Res,* **19,** 600-606.

Kimura T, Okada M, Ishida H (1979) Kinesiological characteristics of primate walking: its significance in human walking. In *Environment, Behavior and Morphology: Dynamic Interactions in Primates* (eds Morbeck ME, Preuschoft H, Gomberg N), pp. 297-311. New York: G. Fischer.

Kivell TL (2016) A review of trabecular bone functional adaptation: what have we learned from trabecular analyses in extant hominoids and what can we apply to fossils? *J Anat,* **228,** 569-94.

Kivell TL, Skinner MM, Lazenby R, Hublin J-J (2011) Methodological considerations for analyzing trabecular architecture: an example from the primate hand. *J Anat,* **218,** 209-225.

Kuo S, Desilva JM, Devlin MJ, McDonald G, Morgan EF (2013) The effect of the Achilles tendon on trabecular structure in the primate calcaneus. *Anat Rec,* **296,** 1509-1517.

Lanyon LE (1974) Experimental support for the trajectorial theory of bone structure. *J Bone Joint Surg Br,* **56,** 160-6.

Lazenby RA, Skinner MM, Hublin J-J, Boesch C (2011a) Metacarpal trabecular architecture variation in the chimpanzee (*Pan troglodytes*): Evidence for locomotion and tool-use? *Am J Phys Anthropol,* **144,** 215-225.

Lazenby RA, Skinner MM, Kivell TL, Hublin J-J (2011b) Scaling VOI size in 3D µCT studies of trabecular bone: A test of the over-sampling hypothesis. *Am J Phys Anthropol,* **144,** 196-203.

Lieberman DE (1996) How and why humans grow thin skulls: Experimental evidence for systemic cortical robusticity. *Am J Phys Anthropol,* **101,** 217-236.

Lieberman DE, Pearson OM, Polk JD, Demes B, Crompton AW (2003) Optimization of bone growth and remodeling in response to loading in tapered mammalian limbs. *J Exp Biol,* **206,** 3125-3138.

Lieberman DE, Polk JD, Demes B (2004) Predicting long bone loading from cross-sectional geometry. *Am J Phys Anthropol,* **123,** 156-171.

Lovejoy CO, McCollum MA, Reno PL, Rosenman BA (2003) Developmental biology and human evolution. *Annu Rev Anthrop,* **32,** 85-109.

Luisier B, Dall′Ara E, Pahr DH (2014) Orthotropic HR-pQCT-based FE models improve strength predictions for stance but not for side-way fall loading compared to isotropic QCT-based FE models of human femurs. *J Mech Behav Biomed Mater,* **32,** 287-299.

MacLatchy L, Müller R (2002) A comparison of the femoral head and neck trabecular architecture of *Galago* and *Perodicticus* using micro-computed tomography (µCT). *J Hum Evol,* **43,** 89-105.

Maga M, Kappelman J, Ryan TM, Ketcham RA (2006) Preliminary observations on the calcaneal trabecular microarchitecture of extant large-bodied hominoids. *Am J Phys Anthropol,* **129,** 410-417.

Maquer G, Musy SN, Wandel J, Gross T, Zysset PK (2015) Bone volume fraction and fabric anisotropy are better determinants of trabecular bone stiffness than other morphological variables. *J Bone Miner Res,* **30,** 1000-1008.
Martin RB, Burr DB, Sharkey NA (1998) *Skeletal Tissue Mechanics,* Springer-Verlag, New York.
McCabe L, Britton R, Parameswaran N (2015) Prebiotic and Probiotic Regulation of Bone Health: Role of the Intestine and its Microbiome. *Curr Osteoporos Rep***,** 1-9.
Morgan EF, Keaveny TM (2001) Dependence of yield strain of human trabecular bone on anatomic site. *J Biomech,* **34,** 569-577.
Mori T, Okimoto N, Sakai A, et al. (2003) Climbing exercise increases bone mass and trabecular bone turnover through transient regulation of marrow osteogenic and osteoclastogenic potentials in mice. *J Bone Miner Res,* **18,** 2002-2009.
Myatt JP, Crompton RH, Thorpe SK (2011) A new method for recording complex positional behaviours and habitat interactions in primates. *Folia Primatol,* **82,** 13-24.
Nguyen NH, Pahr DH, Gross T, Skinner MM, Kivell TL (2014) Micro-finite element (mu FE) modeling of the siamang (*Symphalangus syndactylus*) third proximal phalanx: The functional role of curvature and the flexor sheath ridge. *J Hum Evol,* **67,** 60-75.
Parkinson IH, Fazzalari NL (2003) Interrelationships between structural parameters of cancellous bone reveal accelerated structural change at low bone volume. *J Bone Miner Res,* **18,** 2200-2205.
Pettersson U, Nilsson M, Sundh V, Mellström D, Lorentzon M (2010) Physical activity is the strongest predictor of calcaneal peak bone mass in young Swedish men. *Osteoporos Int,* **21,** 447-455.
Pontzer H, Lieberman DE, Momin E, et al. (2006) Trabecular bone in the bird knee responds with high sensitivity to changes in load orientation. *J Exp Biol,* **209,** 57-65.
Prentice A (1997) Is nutrition important in osteoporosis? *Proc Nutr Soc,* **56,** 357-367.
R Core Team (2016) R: A language and environment for statistical computing. *R Foundation for Statistical Computing*, Vienna, Austria,.
Reginster JY, Burlet N (2006) Osteoporosis: a still increasing prevalence. *Bone,* **38,** S4-9.
Richmond BG (2007) Biomechanics of phalangeal curvature. *J Hum Evol,* **53,** 678-690.
Richmond BG, Wright BW, Grosse I, et al. (2005) Finite element analysis in functional morphology. *Anat Rec,* **283A,** 259-274.
Riggs BL, Melton LJ, 3rd (1995) The worldwide problem of osteoporosis: insights afforded by epidemiology. *Bone,* **17,** 505S-511S.
Robling AG, Hinant FM, Burr DB, Turner CH (2002) Improved bone structure and strength after long-term mechanical loading is greatest if loading is separated into short bouts. *J Bone Miner Res,* **17,** 1545-1554.
Rubin CT, Lanyon LE (1985) Regulation of bone mass by mechanical strain magnitude. *Calcif Tissue Int,* **37,** 411-7.
Ruff CB (1988) Hindlimb articular surface allometry in hominoidea and *Macaca*, with comparisons to diaphyseal scaling. *J Hum Evol,* **17,** 687-714.
Ruff CB (2002) Long bone articular and diaphyseal structure in old world monkeys and apes. I: Locomotor effects. *Am J Phys Anthropol,* **119,** 305-342.
Ruff CB, Burgess ML, Bromage TG, Mudakikwa A, McFarlin SC (2013) Ontogenetic changes in limb bone structural proportions in mountain gorillas (*Gorilla beringei beringei*). *J Hum Evol,* **65,** 693-703.
Ruff CB, Holt B, Trinkaus E (2006) Who's afraid of the big bad Wolff?: "Wolff's law" and bone functional adaptation. *Am J Phys Anthropol,* **129,** 484-498.
Ruff CB, Runestad JA (1992) Primate limb bone structural adaptations. *Annu Rev Anthrop,* **21,** 407-433.
Ryan TM, Ketcham RA (2002a) Femoral head trabecular bone structure in two omomyid primates. *J Hum Evol,* **43,** 241-263.
Ryan TM, Ketcham RA (2002b) The three-dimensional structure of trabecular bone in the femoral head of strepsirrhine primates. *J Hum Evol,* **43,** 1-26.

Ryan TM, Ketcham RA (2005) Angular orientation of trabecular bone in the femoral head and its relationship to hip joint loads in leaping primates. *J Morphol,* **265,** 249-263.

Ryan TM, Krovitz GE (2006) Trabecular bone ontogeny in the human proximal femur. *J Hum Evol,* **51,** 591-602.

Ryan TM, Shaw CN (2012) Unique suites of trabecular bone features characterize locomotor behavior in human and non-human anthropoid primates. *PLoS ONE,* **7,** e41037.

Ryan TM, Shaw CN (2013) Trabecular bone microstructure scales allometrically in the primate humerus and femur. *Proc Biol Sci,* **280**.

Ryan TM, Shaw CN (2015) Gracility of the modern *Homo sapiens* skeleton is the result of decreased biomechanical loading. *Proc Natl Acad Sci U S A,* **112,** 372-377.

Ryan TM, van Rietbergen B (2005) Mechanical significance of femoral head trabecular bone structure in Loris and Galago evaluated using micromechanical finite element models. *Am J Phys Anthropol,* **126,** 82-96.

Ryan TM, Walker A (2010) Trabecular bone structure in the humeral and femoral heads of anthropoid primates. *Anat Rec,* **293,** 719-729.

Saers JPP, Cazorla-Bak Y, Shaw CN, Stock JT, Ryan TM (2016) Trabecular bone structural variation throughout the human lower limb. *J Hum Evol,* **97,** 97-108.

Saparin P, Scherf H, Hublin JJ, Fratzl P, Weinkamer R (2011) Structural adaptation of trabecular bone revealed by position resolved analysis of proximal femora of different primates. *Anat Rec,* **294,** 55-67.

Sarringhaus LA, MacLatchy LM, Mitani JC (2014) Locomotor and postural development of wild chimpanzees. *J Hum Evol,* **66,** 29-38.

Sarringhaus LA, MacLatchy LM, Mitani JC (2016) Long bone cross-sectional properties reflect changes in locomotor behavior in developing chimpanzees. *Am J Phys Anthropol,* **160,** 16-29.

Scherf H (2008) Locomotion-related femoral trabecular architectures in primates: High resolution computed tomographies and their implications for estimations of locomotor preferences of fossil primates. In *Anatomical Imaging* (eds Endo H, Frey R), pp. 39-59. Springer Japan.

Scherf H, Harvati K, Hublin JJ (2013) A comparison of proximal humeral cancellous bone of great apes and humans. *J Hum Evol,* **65,** 29-38.

Scherf H, Tilgner R (2009) A new high-resolution computed tomography (CT) segmentation method for trabecular bone architectural analysis. *Am J Phys Anthropol,* **140,** 39-51.

Scherf H, Wahl J, Hublin J-J, Harvati K (2015) Patterns of activity adaptation in humeral trabecular bone in Neolithic humans and present-day people. *Am J Phys Anthropol,* **159,** 106-15.

Schilling AM, Tofanelli S, Hublin JJ, Kivell TL (2014) Trabecular bone structure in the primate wrist. *J Morphol,* **275,** 572-85.

Schneider CA, Rasband WS, Eliceiri KW (2012) NIH Image to ImageJ: 25 years of image analysis. *Nat Methods,* **9,** 671-675.

Shaw CN, Ryan TM (2012) Does skeletal anatomy reflect adaptation to locomotor patterns? Cortical and trabecular architecture in human and nonhuman anthropoids. *Am J Phys Anthropol,* **147,** 187-200.

Shea B, Wells G, Cranney A, et al. (2002) Meta-analyses of therapies for postmenopausal osteoporosis. VII. Meta-analysis of calcium supplementation for the prevention of postmenopausal osteoporosis. *Endocr Rev,* **23,** 552-9.

Skedros JG, Baucom SL (2007) Mathematical analysis of trabecular 'trajectories' in apparent trajectorial structures: The unfortunate historical emphasis on the human proximal femur. *J Theor Biol,* **244,** 15-45.

Skerry TM, Lanyon LE (1995) Interruption of disuse by short duration walking exercise does not prevent bone loss in the sheep calcaneus. *Bone,* **16,** 269-274.

Skinner MM, Stephens NB, Tsegai ZJ, et al. (2015) Human-like hand use in *Australopithecus africanus*. *Science,* **347,** 395-399.

Smith RJ, Jungers WL (1997) Body mass in comparative primatology. *J Hum Evol,* **32,** 523-59.

Sode M, Burghardt AJ, Nissenson RA, Majumdar S (2008) Resolution dependence of the non-metric trabecular structure indices. *Bone,* **42,** 728-36.

Stauber M, Rapillard L, van Lenthe GH, Zysset P, Müller R (2006) Importance of individual rods and plates in the assessment of bone quality and their contribution to bone stiffness. *J Bone Miner Res,* **21,** 586-595.

Stephens NB, Kivell TL, Gross T, et al. (2016) Trabecular architecture in the thumb of Pan and Homo: implications for investigating hand use, loading, and hand preference in the fossil record. *Am J Phys Anthropol,* **161,** 603-619.

Strait DS, Wang Q, Dechow PC, et al. (2005) Modeling elastic properties in finite-element analysis: How much precision is needed to produce an accurate model? *Anat Rec,* **283A,** 275-287.

Su A (2011) *The Functional Morphology of Subchondral and Trabecular Bone in the Hominoid Tibiotalar Joint.* (Doctoral Dissertaion). Stony Brook University.

Su A, Carlson KJ (2017) Comparative analysis of trabecular bone structure and orientation in South African hominin tali. *J Hum Evol,* **106,** 1-18.

Su A, Wallace IJ, Nakatsukasa M (2013) Trabecular bone anisotropy and orientation in an Early Pleistocene hominin talus from East Turkana, Kenya. *J Hum Evol,* **64,** 667-677.

Susman RL, Badrian NL, Badrian AJ (1980) Locomotor behavior of *Pan paniscus* in Zaire. *Am J Phys Anthropol,* **53,** 69-80.

Tanck E, Homminga J, van Lenthe GH, Huiskes R (2001) Increase in bone volume fraction precedes architectural adaptation in growing bone. *Bone,* **28,** 650-654.

Thorpe SK, Crompton RH (2006) Orangutan positional behavior and the nature of arboreal locomotion in Hominoidea. *Am J Phys Anthropol,* **131,** 384-401.

Tsegai ZJ, Kivell TL, Gross T, et al. (2013) Trabecular bone structure correlates with hand posture and use in hominoids. *PLoS ONE,* **8,** e78781.

Tsegai ZJ, Skinner MM, Gee AH, et al. (2017) Trabecular and cortical bone structure of the talus and distal tibia in *Pan* and *Homo*. *Am J Phys Anthropol*.

Ulrich D, van Rietbergen B, Laib A, Ruegsegger P (1999) The ability of three-dimensional structural indices to reflect mechanical aspects of trabecular bone. *Bone,* **25,** 55-60.

Wallace IJ, Kwaczala AT, Judex S, Demes B, Carlson KJ (2013) Physical activity engendering loads from diverse directions augments the growing skeleton. *J Musculoskelet Neuronal Interact,* **13,** 283-8.

Wallace IJ, Pagnotti GM, Rubin-Sigler J, et al. (2015) Focal enhancement of the skeleton to exercise correlates with responsivity of bone marrow mesenchymal stem cells rather than peak external forces. *J Exp Biol,* **218,** 3002-3009.

Wallace IJ, Tommasini SM, Judex S, Garland T, Jr., Demes B (2012) Genetic variations and physical activity as determinants of limb bone morphology: an experimental approach using a mouse model. *Am J Phys Anthropol,* **148,** 24-35.

Wickham H (2009) *ggplot2: Elegant graphics for data analysis,* Springer-Verlag, New York.

Wolff J (1986) *The Law of Bone Remodelling,* Springer, Berlin.

Zeininger A, Patel BA, Zipfel B, Carlson KJ (2016) Trabecular architecture in the StW 352 fossil hominin calcaneus. *J Hum Evol,* **97,** 145-158.

Tables

Table 1. Study sample

Taxon	Collection[1]	Specimen ID	Sex	Elements
H. sapiens	UG	INDEN_91	M	R Hum, R MC3 R Fem, R Tib, R Tal, L MT3 T1
H. sapiens	UG	INDEN_113	M?	R Hum, L MC3 R Fem, L Tib, L Tal, L MT3 T1
H. sapiens	UG	INDEN_118	F	R Hum, R MC3 R Fem, L Tib, L Tal, L MT3 T1
H. sapiens	UG	INDEN_311	M	R Hum, R MC3 R Fem, L Tib, L Tal, R MT3 T1
H. sapiens	UK	NGA_88_SK_766	U	L Hum, L MC3 R Fem, R Tib, R Tal, R MT3 T1
H. sapiens	UK	NGA_88_SK_825	U	R Hum, R MC3 L Fem, L Tib, R Tal, R MT3 T1
H. sapiens	UK	NGA_88_SK_880	U	R Hum, R MC3 L Fem, L Tib, L Tal, L MT3 T1
P. troglodytes verus	MPIEVA	MPITC_11781	M	L Hum, L MC3 R Fem, R Tib, R Tal, R MT3 T1
P. troglodytes verus	MPIEVA	MPITC_11778	F	L Hum, L MC3 R Fem, R Tib, R Tal, R MT3 T1
P. troglodytes verus	MPIEVA	MPITC_14996	F	L Hum, L MC3 R Fem, R Tib, R Tal, R MT3 T1
P. troglodytes verus	MPIEVA	MPITC_15001	F	L Hum, L MC3 R Fem, R Tib, R Tal, R MT3 T1
P. troglodytes verus	MPIEVA	MPITC_15002	F	L Hum, L MC3 R Fem, R Tib, R Tal, R MT3 T1
P. troglodytes verus	MPIEVA	MPITC_15012	M	R Hum, L MC3 R Fem, R Tib, R Tal, L MT3 T1
P. troglodytes verus	MPIEVA	MPITC_15013	F	L Hum, L MC3 R Fem, R Tib, L Tal, R MT3 T1

[1] MPIEVA – Max Planck Institute for Evolutionary Anthropology, UK – University of Kent, UG – University of Göttingen

[2] M – Male, F – Female, U – Unknown, ? – indicates uncertainty concerning sex. Data taken from collection records.

Table 2. Trabecular structure in each taxon across anatomical sites. Mean values with standard deviation in parentheses, and p-values resulting from Mann-Whitney U tests between taxa. Significant differences are shown in bold.

Element	Taxon	Tb.Th (mm)	BV/TV (%)	DA
Humerus	*Homo*	0.21 (0.02)	12.72 (4.07)	0.11 (0.04)
	Pan	0.22 (0.02)	25.32 (3.82)	0.17 (0.02)
	p-value	0.90	**<0.01**	**<0.01**
MC3	*Homo*	0.19 (0.02)	21.25 (3.16)	0.20 (0.08)
	Pan	0.18 (0.01)	22.75 (1.58)	0.23 (0.04)
	p-value	0.32	0.16	0.46
T1	*Homo*	0.22 (0.04)	21.29 (5.91)	0.12 (0.05)
	Pan	0.20 (0.02)	26.08 (3.78)	0.18 (0.05)
	p-value	0.38	0.16	**0.03**
Femur	*Homo*	0.26 (0.03)	22.72 (5.45)	0.16 (0.05)
	Pan	0.33 (0.07)	38.58 (6.85)	0.08 (0.09)
	p-value	0.07	**<0.01**	0.13
Tibia	*Homo*	0.26 (0.02)	21.66 (3.11)	0.29 (0.06)
	Pan	0.24 (0.03)	25.98 (4.31)	0.34 (0.05)
	p-value	0.16	0.10	0.05
Talus	*Homo*	0.27 (0.03)	26.26 (3.43)	0.11 (0.06)
	Pan	0.31 (0.04)	35.94 (3.87)	0.02 (0.03)
	p-value	0.07	**<0.01**	**<0.01**
MT3	*Homo*	0.17 (0.02)	17.54 (3.47)	0.31 (0.03)
	Pan	0.18 (0.03)	22.89 (3.93)	0.22 (0.03)
	p-value	0.90	**0.01**	**<0.01**

Table 3. Comparisons of trabecular structure between anatomical sites within each taxon. Mean rank of each trabecular variable within individuals from lowest (1) to highest (7) in *Homo* and *Pan*. Results of Friedman tests indicate the presence of significant differences between anatomical sites in *Homo* and in *Pan*. Significant differences are shown in bold.

		Rank		
Taxon	Element	Tb.Th	BV/TV	DA
Homo	Humerus	3.43	1.00	2.29
	MC3	2.29	4.29	4.57
	T1	3.57	4.43	2.43
	Femur	5.71	5.14	3.71
	Tibia	6.00	4.29	6.14
	Talus	6.00	6.57	2.29
	MT3	1.00	2.29	6.57
	p-value	**<0.01**	**<0.01**	**<0.01**
Pan	Humerus	3.57	3.57	3.29
	MC3	2.14	2.00	5.29
	T1	3.00	3.71	3.86
	Femur	6.57	6.85	2.57
	Tibia	4.86	4.00	6.86
	Talus	6.43	6.14	1.00
	MT3	1.43	1.71	5.14
	p-value	**<0.01**	**<0.01**	**<0.01**

Table 4. Comparison between anatomical regions within each taxon. P-values from pairwise Wilcoxon tests with a post-hoc Bonferroni correction between all anatomical sites in *Homo* (shaded) and *Pan* (unshaded). Significant differences are shown in bold.

		Humerus	MC3	T1	Femur	Tibia	Talus	MT3
Tb.Th	Humerus		0.146	1.000	0.086	**0.049**	**0.024**	**0.012**
	MC3	**0.024**		1.000	**0.012**	**0.012**	**0.012**	1.000
	T1	1.000	0.795		1.000	0.233	0.367	0.795
	Femur	**0.049**	**0.012**	**0.024**		1.000	1.000	**0.012**
	Tibia	1.000	**0.012**	0.795	0.551		1.000	**0.012**
	Talus	**0.012**	**0.012**	**0.012**	1.000	0.147		**0.012**
	MT3	0.367	1.000	1.000	**0.024**	0.086	**0.012**	
BV/TV	Humerus		0.086	0.147	**0.049**	0.086	**0.012**	0.551
	MC3	1.000		1.000	1.000	1.000	0.367	0.367
	T1	1.000	0.795		1.000	1.000	1.000	1.000
	Femur	0.086	**0.012**	**0.049**		1.000	1.000	1.000
	Tibia	1.000	1.000	1.000	0.086		0.795	0.367
	Talus	**0.012**	**0.012**	**0.024**	1.000	**0.024**		0.086
	MT3	1.000	1.000	1.000	**0.024**	1.000	**0.012**	
DA	Humerus		0.551	1.000	1.000	**0.012**	1.000	**0.012**
	MC3	**0.049**		0.551	1.000	1.000	0.551	**0.024**
	T1	1.000	1.000		1.000	**0.012**	1.000	**0.012**
	Femur	1.000	0.147	1.000		0.233	1.000	**0.012**
	Tibia	**0.012**	0.086	**0.024**	**0.012**		**0.012**	1.000
	Talus	**0.012**	**0.012**	**0.012**	0.795	**0.012**		**0.012**
	MT3	0.086	1.000	1.000	0.551	**0.049**	**0.012**	

Figure legends

Figure 1. Region of interest defined for each element. Grey boxes represent the definition of each region in specimens of *Pan* for (A) humeral head, (B) femoral head, (C) distal tibia, (D) third metacarpal head, (E) third metatarsal head, and (F) first thoracic vertebral body (shown in a mid-sagittal section, as transverse process obscures a clear view of the vertebral body). For the talus, not shown here, trabecular structure was quantified throughout the entire bone.

Figure 2. Quantification of trabecular bone. (A) Segmented voxel data where cortex, trabecular bone and air inside the bone are assigned different grey values. (B) Trabecular only region which was imported into BoneJ to measure Tb.Th. (C) 3D tetrahedral mesh of cortex and inner region of bone. (D) Each element in the tetrahedral mesh of the inner region was assigned a BV/TV value, as visualised here where regions of low BV/TV are in blue and high BV/TV in red.

Figure 3. Variation in trabecular bone structure across the skeleton of *Homo* and *Pan*. Boxplots showing (A) Tb.Th, (B) BV/TV and (C) DA in the humeral head (Hum), third metacarpal head (MC3), femoral head (Fem), distal tibia (Tib), talus (Tal), third metatarsal head (MT3), and first thoracic vertebra (T1) in *Homo* (red) and *Pan* (blue). Significant differences are indicated by brackets with * for $p<0.05$ and ** for $p<0.01$.

Figure 4. Systemic differences in BV/TV across the skeleton of *Homo* (red) and *Pan* (blue). BV/TV in each individual of *Homo* (red) and *Pan* (blue) in the humeral head (Hum), third metacarpal head (MC3), femoral head (Fem), distal tibia (Tib), talus (Tal), third metatarsal head (MT3), and first thoracic vertebra (T1)

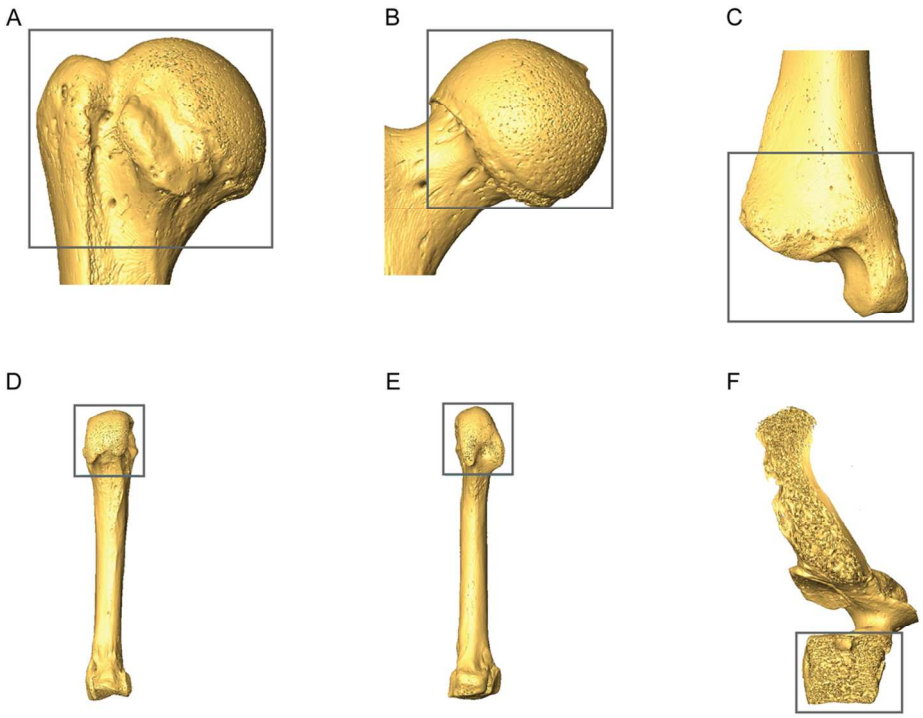

Figure 1

110x80mm (300 x 300 DPI)

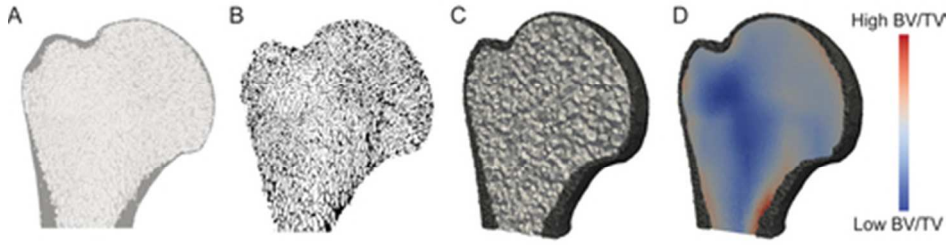

Figure 2

39x10mm (300 x 300 DPI)

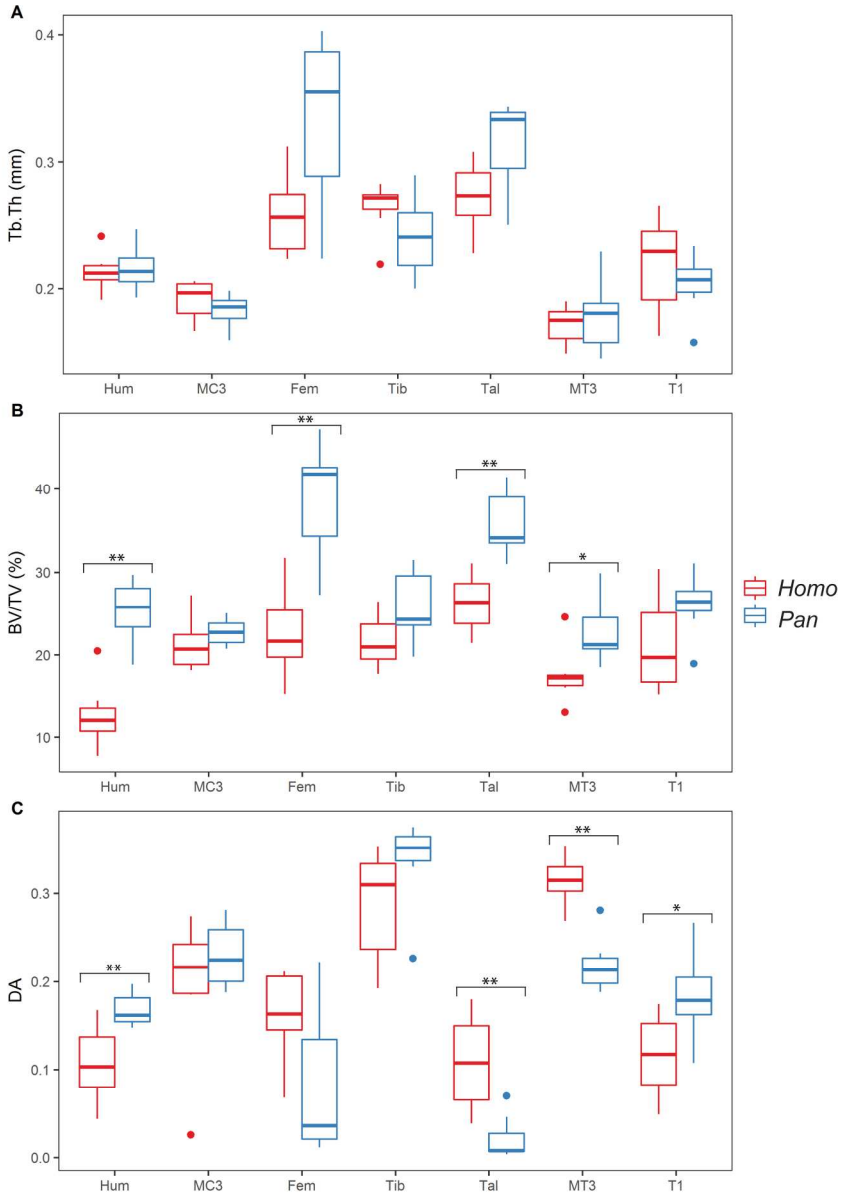

Figure 3

208x295mm (300 x 300 DPI)

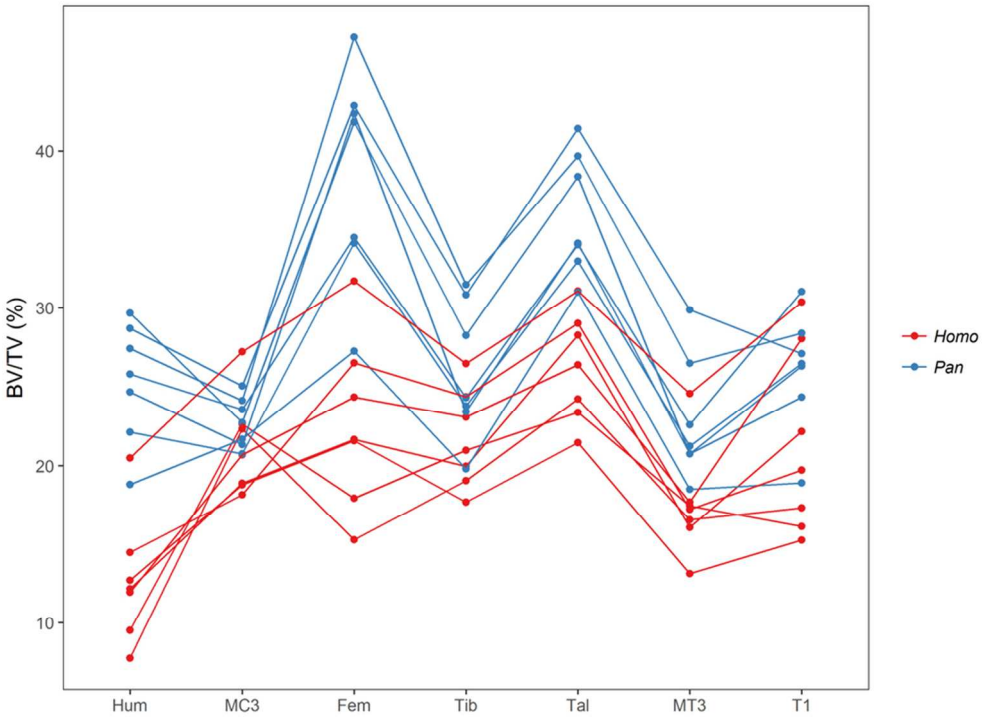

Figure 4

87x63mm (300 x 300 DPI)